This is the author's version of a work that was accepted for publication in the following source:

Sikder, M. K. U., M. N. Shivdasani, J. B. Fallon, P. Seligman, K. Ganesan, J. Villalobos, S. Prawer, and D. J. Garrett. 2019. Electrically conducting diamond films grown on platinum foil for neural stimulation. *Journal of Neural Engineering*. **16**(6): 066002.

doi: 10.1088/1741-2552/ab2e79

Notice: Changes introduced as a result of publishing processes such as copy-editing and formatting may not be reflected in this document. For a definitive version of this work, please refer to the published source.

The final publication is available here

Copyright of this article belongs to: © 2019 IOP Publishing Ltd

Journal of Neural Engineering

ACCEPTED MANUSCRIPT

Electrically conducting diamond films grown on platinum foil for neural stimulation

To cite this article before publication: Md Kabir Uddin Sikder *et al* 2019 *J. Neural Eng.* in press https://doi.org/10.1088/1741-2552/ab2e79

Manuscript version: Accepted Manuscript

Accepted Manuscript is "the version of the article accepted for publication including all changes made as a result of the peer review process, and which may also include the addition to the article by IOP Publishing of a header, an article ID, a cover sheet and/or an 'Accepted Manuscript' watermark, but excluding any other editing, typesetting or other changes made by IOP Publishing and/or its licensors"

This Accepted Manuscript is **© 2019 IOP Publishing Ltd**.

During the embargo period (the 12 month period from the publication of the Version of Record of this article), the Accepted Manuscript is fully protected by copyright and cannot be reused or reposted elsewhere.
As the Version of Record of this article is going to be / has been published on a subscription basis, this Accepted Manuscript is available for reuse under a CC BY-NC-ND 3.0 licence after the 12 month embargo period.

After the embargo period, everyone is permitted to use copy and redistribute this article for non-commercial purposes only, provided that they adhere to all the terms of the licence https://creativecommons.org/licences/by-nc-nd/3.0

Although reasonable endeavours have been taken to obtain all necessary permissions from third parties to include their copyrighted content within this article, their full citation and copyright line may not be present in this Accepted Manuscript version. Before using any content from this article, please refer to the Version of Record on IOPscience once published for full citation and copyright details, as permissions will likely be required. All third party content is fully copyright protected, unless specifically stated otherwise in the figure caption in the Version of Record.

View the article online for updates and enhancements.

This content was downloaded from IP address 128.250.144.144 on 23/07/2019 at 05:56

IOP Publishing Journal Title
Journal **XX** (XXXX) XXXXXX https://doi.org/XXXX/XXXX

Electrically conducting diamond films grown on platinum foil for neural stimulation

Md. Kabir Uddin Sikder[1,4], Mohit N. Shivdasani [2,3], James B. Fallon[3,5], Peter Seligman[3], Kumaravelu Ganesan[6], Joel Villalobos[3], Steven Prawer[6], and David J. Garrett[*,6]

[1]Department of Medical Bionics, The University of Melbourne, Parkville, Melbourne, VIC 3010, Australia
[2]Graduate School of Biomedical Engineering, The University of New South Wales Kensington, NSW 2033, Australia
[3]Bionics Institute, 384 Albert St, East Melbourne, VIC 3002, Australia
[4]Department of Physics, Jahangirnagar University, Savar, Dhaka 1342, Bangladesh
[5]Department of Otolaryngology, The University of Melbourne, Parkville, Melbourne, VIC 3010, Australia
[6]School of Physics, The University of Melbourne, Parkville, Melbourne, VIC 3010, Australia
* Corresponding Author

E-mail: dgarrett@unimelb.edu.au

Received xxxxxx
Accepted for publication xxxxxx
Published xxxxxx

Abstract

Objective

With the strong drive towards miniaturization of active implantable medical devices and the need to improve the resolution of neural stimulation arrays, there is keen interest in the manufacture of small electrodes capable of safe, continuous stimulation. Traditional materials such as platinum do not possess the necessary electrochemical properties to stimulate neurons safely when electrodes are very small (i.e. typically less than about 300 um (78400 μm^2)). While there are several commercially viable alternative electrode materials such as titanium nitride and iridium oxide, an attractive approach is modification of existing Pt arrays via a high electrochemical capacitance material coating. Such a composite electrode could still take advantage of the wide range of fabrication techniques used to make platinum-based devices. The coating, however, must be biocompatible, exhibit good adhesion and ideally be long lasting when implanted in the body.

Approach

Platinum foils were roughened to various degrees with regular arrays of laser milled pits. Conducting diamond films were grown on the foils by microwave plasma chemical vapor deposition. The adhesion strength of the films to the platinum was assessed by prolonged sonication and accelerated aging. Electrochemical properties were evaluated and compared to previous work.

Main results

In line with previous results, diamond coatings increased the charge injection capacity of the platinum foil by more than 300% after functionalization within an oxygen plasma. Roughening of the underlying platinum substrate by laser milling was required to generate strong adhesion between the diamond and the Pt foil. Electrical stress testing, near the limits of safe operation, showed that the diamond films were more electrochemically stable than platinum controls.

Significance

Accepted Manuscript

 © xxxx IOP Publishing Ltd

IOP Publishing Journal Title
Journal **XX** (XXXX) XXXXXX https://doi.org/XXXX/XXXX

The article describes a new method to protect platinum electrodes from degradation *in vivo.* A 300% increase in charge injection means that device designers can safely employ diamond coated platinum stimulation electrodes at much smaller sizes and greater density than is possible for platinum.

Keywords: Diamond, Electrode, Neural Stimulation, Medical Implant, capacitance, coating, platinum

1. Introduction

Recent investment by major medical manufacturers, governments and startup companies indicates that bionic implants are set to enjoy an increasing role in the future of medicine. Implantable monitoring and recording devices will represent a major part of this industry but neural stimulation implants are likely to enjoy growth and find application in a variety of new and established markets. Since the success of pacemakers and cochlear implants for deafness, implantable electrical stimulators for modulation of the human nervous system have become commonplace. Applications include deep brain stimulators for Parkinson's disease [1], post-traumatic stress disorder (PTSD) [2] and traumatic brain injury [3]; implants for restoration of hearing (cochlear) and sight (retinal prosthetics); stimulators for drug-resistant epilepsy, nerve stimulators for pain control and vagus nerve stimulators [4], to regulate the body's own biochemical processes (i.e. the field of electroceuticals).

The majority of neurostimulation devices currently on the market, feature mm scale electrodes and interface with the central or peripheral nervous system at low resolution. Deep brain stimulator electrodes, for instance, feature only a few large electrodes, millimeters in diameter [5]. Devices designed to restore lost human sensation are also available. The cochlear implant to restore hearing led the way [6] but retinal stimulators to restore vision are now a market reality [7]. Together with the burgeoning field of brain-machine interfaces [8], these implants illustrate the need to interact with neurons in a much more sophisticated way and at much higher spatial resolutions than has previously been necessary. Hence, there has been in a shift in the focus of implant research towards miniaturization, development of wireless communication and power delivery, increasingly sophisticated neural stimulation strategies and denser multielectrode arrays.

From a safety point of view, stimulation electrodes must inject enough charge to activate neurons without the electrode experiencing dangerous voltages. In electrical terms, the parameter that governs this ability is electrochemical capacitance. Capacitance is the voltage rise experienced in response to the storage of a certain quantity of charge, expressed in Coulombs per volt (C/V) or farads (F). In neural stimulation, charge injection capacity (Q_{inj}) is a figure of merit used to compare materials. It is defined as the maximum amount of charge that can be stored at the electrode-tissue interface, per unit area before voltages exceed a predetermined limit and are expressed in C/cm^2 [9]. Usually, the predetermined voltage limit is the voltage magnitude before water splitting (reduction or oxidation of water) is observed. We have previously established water window limits for N-UNCD from cyclic voltammetry [10, 11]. For the purposes of this work, we use the most conservative of our upper voltage limits, +1 V. Q_{inj} can be expressed as

$$Q_{inj} = C/A \times V_{max}$$

where C = electrode capacitance , A = geometric electrode area, and V_{max} = maximum safe electrode voltage.

Platinum remains the most popular material for fabrication of neural stimulation electrodes in medical devices [12, 13]. In addition to being a noble metal, it is biocompatible, weldable, ductile, has reasonable conductivity, a relatively high Q_{inj} for a metal (0.05 – 0.15 $mCcm^{-2}$ [12]), and it has an established pedigree of use in successful

 © xxxx IOP Publishing Ltd

Accepted Manuscript

clinical applications including the cochlear implant, DBS systems, and retinal prostheses. Increasingly, however, the drive to make high-resolution neural stimulation electrode arrays has led to a need for very small electrodes. Corna *et al* [14] in a review on the subject, discovered that charge density for stimulation of retinal ganglion cells was stable for electrodes greater than 78400 μm^2 (approximately 320 µm in diameter), but increased dramatically below that limit. Well over 1 mC/cm^2 was required for several of the small electrodes reviewed, much greater than the safety limits deliverable through conventional materials. Cogan et al, in a review of stimulation safety limits [15] illustrates that this phenomenon is likely tied to the behavior of microelectrodes which, electrochemically speaking, tend to behave as point sources (far-field stimulators) rather than near-field. Hence, for very small electrodes, accepted stimulation safety limits, such as the Shannon limit [16], may not apply [15]. The consequence for microelectrodes is that conventional materials, such as platinum, do not possess sufficient charge injection capacity to be safe at very small dimensions, hence alternative materials are sought.

Increasing the electrochemical capacitance of metal electrodes is typically accomplished either by roughening the electrode surface [17] or adding a coating. A variety of materials that fulfill this role have risen to the fore including iridium oxide, platinum black, titanium nitride, hydrogels [18] and a range of exotic conducting polymers [19]. Because these devices are implanted into the body and interact directly with neural tissue, they must be biocompatible. In practice, there is a very short list of materials that are considered safe inside the body. The list of materials that are also biostable and long lasting is even shorter. Not only must stimulation electrodes possess high biocompatibility and biostability, they must also adhere to strict electrochemical guidelines in order to spare neural tissue from electrically-induced damage.

Diamond is a material that exhibits excellent biocompatibility [20] and is famously chemically inert and long-lasting. We have previously demonstrated that films of nitrogen included nanocrystalline diamond (N-UNCD) can be used for hermetic encapsulation [21] and can be post-treated with oxygen plasma yielding Q_{inj} values as high as 1.2 $mCcm^{-2}$ [10, 22], comparable with leading high injection materials such as iridium oxide or titanium nitride. A number of reports exist demonstrating *in vitro* [11, 23] and *in vivo* [24] neural stimulation with diamond electrodes. In the work described here, our aim was to enhance the electrochemical performance of platinum electrodes by growing a film of N-UNCD and activating that film towards high charge injection capacity. Diamond films have previously been grown on platinum wire [25, 26] and heteroepitaxial films on single crystal platinum [27] and on TEM grids [28] but not on large scale free-standing foils and not for neural stimulation applications.

2. Experimental Details

2.1 Preparation of N-UNCD films on Pt foil.

In build-up work, we discovered that CVD diamond films exhibited extremely poor adhesion to smooth silicon most likely due to platinum not readily forming a carbide. To improve adhesion, 50 um thick platinum foils (Goodfellow, UK) were laser milled with a regular array of pits using an Oxford Laser CNC milling system fitted with a 532 nm, frequency doubled, nanosecond pulsed, YAG laser. Growth of N-UNCD films on platinum was conducted in an IPLAS microwave plasma chemical vapor deposition (MPCVD) system by a previously published process.[10, 11, 21]. Briefly, platinum foils were seeded by sonication in a suspension of 3-5 nm detonation nanodiamonds (Nano armor) in methanol. The seeded foils were dried under a flow of compressed air and transferred to the CVD reactor. The reactor gas mixture was Ar : N_2: CH_4 at a ratio of 79:20:1 % and a chamber pressure of 80 tor. 1000 W of microwave power was supplied to ignite the plasma and a heating stage set to 800 ^oC was used. Films were grown for 3 h resulting in films approximately 3 µm in thickness. The process is depicted in Fig. 1. A subset of samples was subjected to oxygen plasma treatment (termed N-UNCD-O) for 3 h at 0.8 mbar in a plasma cleaner (Electronic Diener, Plasma-Surface-Technology) operating at 50 W with a gas mixture of ratio of 80:20, Ar : O_2.

Accepted Manuscript

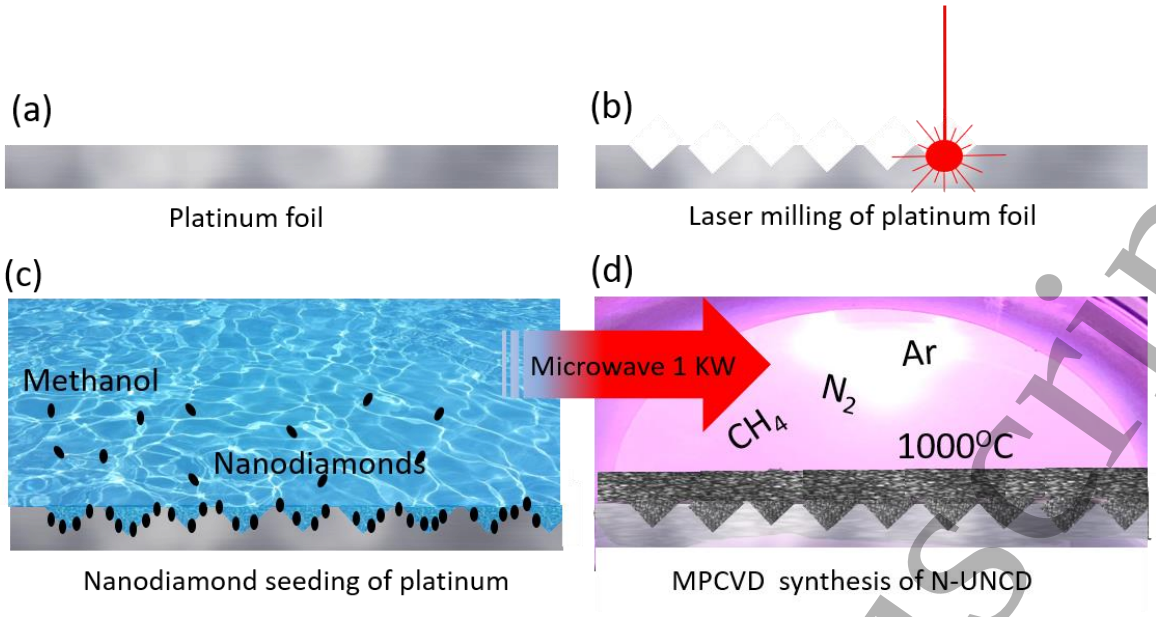

Fig. 1. Process of fabricating films of N-UNCD on laser roughened diamond. (a) Bare platinum foil was laser roughened (b) by drilling a series of pits at a variety of spacings. (c) the roughened platinum foils were seeded with nanodiamonds by sonication in a nanodiamond suspension in methanol. (d) Diamond films were gown on the seeded foils by microwave plasma assisted chemical vapor deposition.

2.2 Characterization of films

Cyclic voltammograms were recorded on a Solartron SI1287 electrochemical interface (potentiostat, Solartron SI1260 impedance/Gain-phase analyzer). Counter electrodes were in-house made platinum mesh and reference electrodes were 1 M Ag/ AgCl (CH Instruments). Pulse tests were delivered by an in-house built constant current stimulator and symmetric biphasic charge-balanced pulses were used. Electrode diameters were either 3 mm, defined by an O-ring, or 1 mm, defined by lithographically patterned SU-8 photoresist. Large electrode areas were used in order to reduce error in measured capacitance values. Current and voltage during pulse tests were measured with a National Instruments (PXI-4072, National Instruments, USA). Charge injection capacity (Q_{inj}) for each electrode type was calculated by dividing the maximum deliverable charge (coulombs) during a stimulation pulse by the electrode geometric area and multiplying by 1 V (Maximum safe voltage, established in previous work [11]). The Q_{inj} for all electrodes before and after electrochemical stress testing was measured for a variety of phase durations. Scanning electron microscopy (SEM) of electrodes was conducted at the Advanced Microscopy Facility at Bio21, (The University of Melbourne) on an FEI NOVA Nanolab.

2.3 Mechanical and Electrochemical Stress testing of films.

Samples (plain Pt foil, roughened Pt foil and N-UNCD coated Pt foil) were suspended in distilled/deionized (DI) water and exposed to sonication (Elmasonic P sonicator, 80KHz 100% power) for various lengths of time to establish mechanical stability. Electrochemical stress testing was conducted on 1 mm diameter lithographically patterned electrodes in SU8, fabricated by standard lithographic methods (Fig. 2). All electrodes were subjected to 5 days of constant stimulation at a rate of 50 Hz (400 µs per phase). All samples were stimulated at a current that resulted in a cathodic electrode polarization to their respective maximum safe limits, 0.6 V [12] for platinum and 1.0 V for N-UNCD [11].

Accepted Manuscript

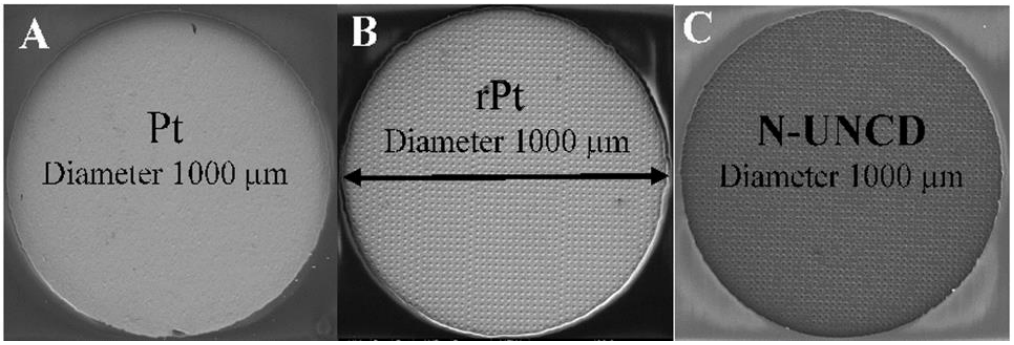

Fig. 2. Lithographically patterned Pt (A), rPt (B) and N-UNCD (C) electrodes in SU-8 photoresist.

3. Results

3.1 Film deposition and mechanical adhesion assessment.

Fig. 3 shows SEM images of platinum foil (A, B, and C) laser milled with 20 µm diameter pits in a regular array pattern with separations of 20, 40 and 80 µm. Fig. 3 D, E and F shows higher magnification images of the same foils after MPCVD growth of N-UNCD which grew conformally over the foil and featured typical, irregular surface morphology with occasional mushroom-like outgrowths.

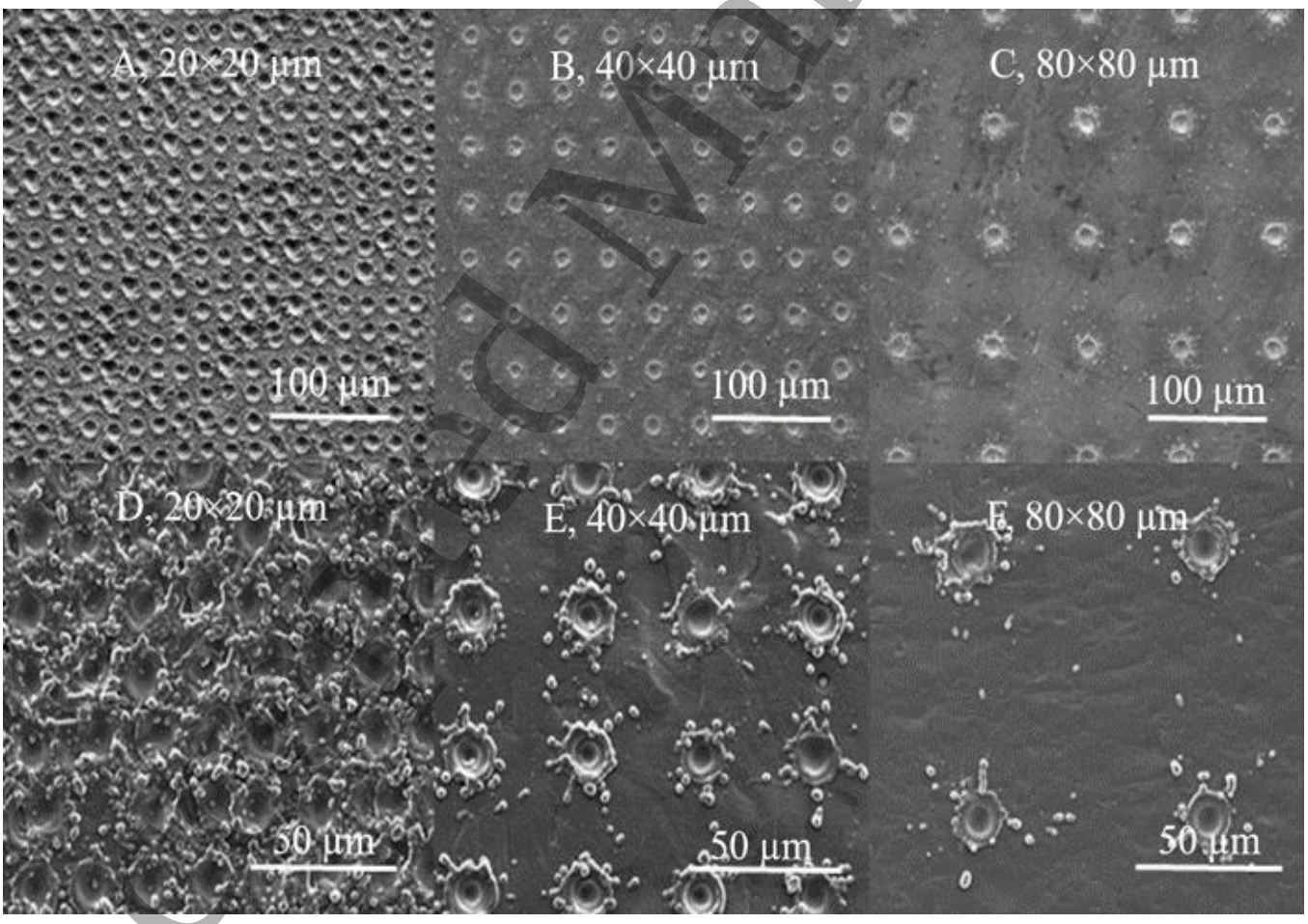

Accepted Manuscript

Fig. 3. SEM images of platinum foil (A, B and C) milled with small pits at 20, 40 and 80 μm spacing. Higher magnification SEM images of N-UNCD films (D, E, and F) grown on the same films depicted in A, B and C.

During sonication in DI water, films laser milled with 40 and 80 μm pit separation exhibited rapid delamination. Fig. 4 shows SEM images of various films, following sonication for various lengths of time. Fig. 4, C1 shows the result of 0.5 h of sonication of an N-UNCD film grown on a foil with 80 μm separation pits. Approximately 50% of the film is delaminated after just 0.5 h, evident by the lighter color of the platinum foil showing through darker color of the diamond film. This sample exhibited almost complete delamination after 15 h (Fig. 4, C4). Adhesion was improved when laser milled pits were spaced at 40 μm with major delamination beginning to occur after 2.5 h of sonication (Fig. 5, B2). By contrast, N-UNCD grown on foils with 20 μm pit separation exhibited minimal delamination over all sonication time periods (Fig. 4, A1-4). The sample shown in Fig. 4, A1-4 was subjected to a further 15 h of sonication to establish whether the small delaminated patch evident on image A4 would become larger. High magnification images of the delaminated patch after 30 h of sonication are shown in Fig. 5. There was no evidence of additional delamination occurring between 15 and 30 h of sonication.

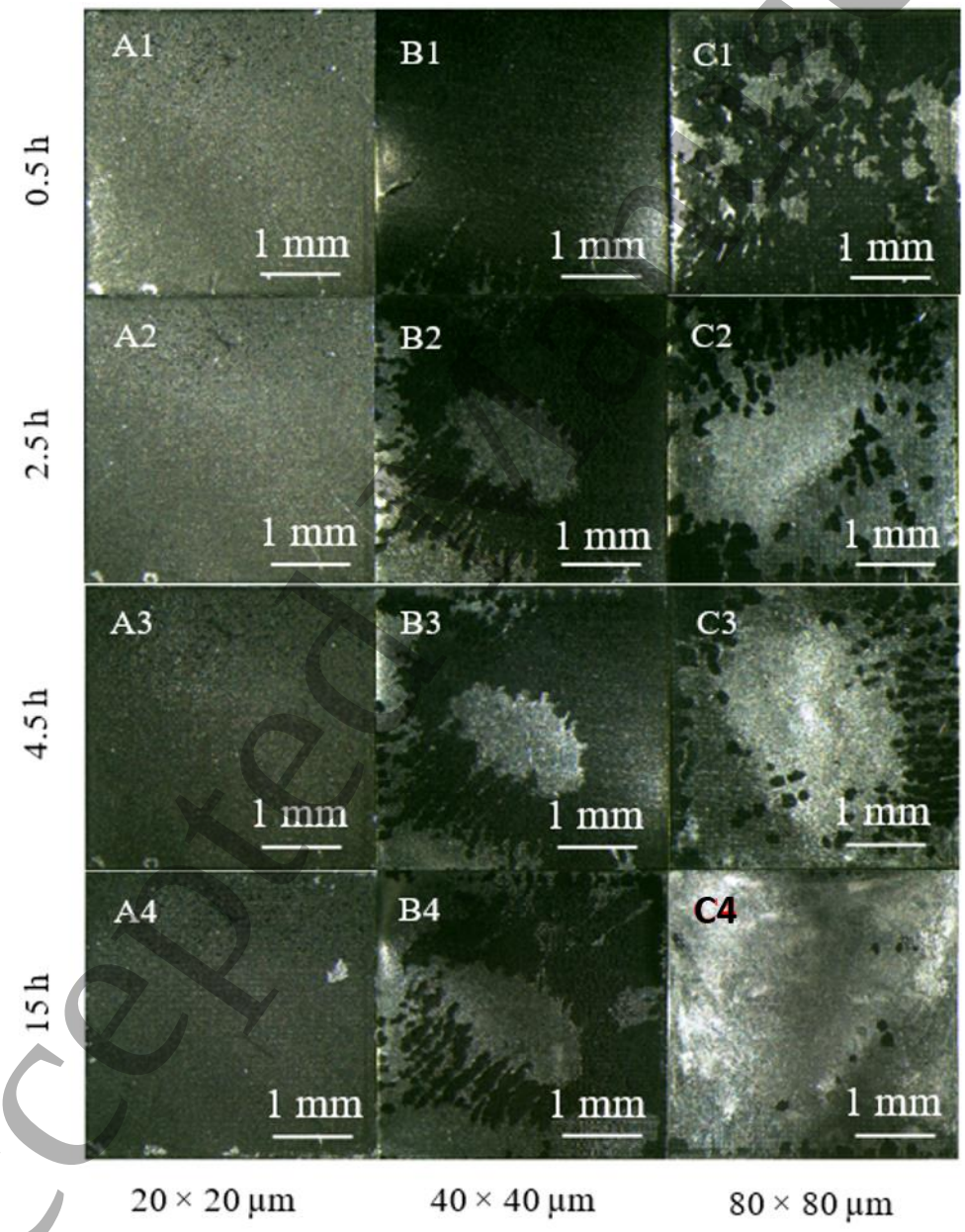

Accepted manuscript

Fig. 4. SEM images of N-UNCD films grown on platinum foil laser milled with holes at 20 (A),40 (B) and 80 (C) µm spacing. The figure shows a progression of SEM images following sonication of the three films, in DI water for 0.5, 2.5, 4.5 and 15 h.

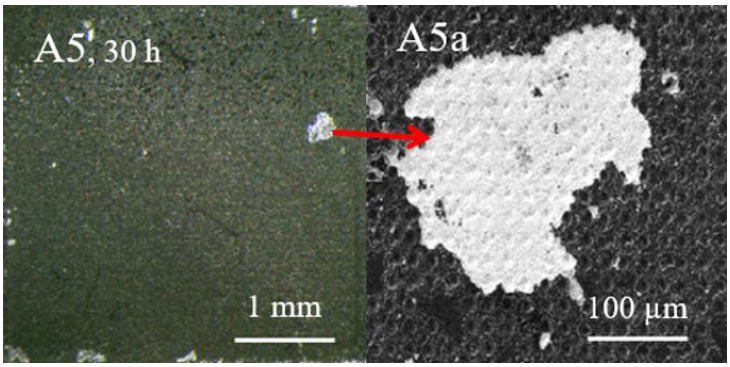

Fig. 5. SEM image of a small delaminated patch apparent in Figure 4 (A4) after an additional 15 h of sonication in DI water (30 h total).

3.2 Electrochemical characterization and stability assessment.

Fig. 6 shows a typical recorded trace (current and voltage) from smooth platinum (Pt, blue trace) foil, 20 µm hole separation laser roughened platinum (rPt, red trace) foil and laser roughened foil after growth of an N-UNCD film (N-UNCD, black trace). The traces were recorded during a typical, constant current stimulation pulse of 400 µs per phase with an interphase gap of 25 µs. Fig. 6, A shows the maximum current amplitude that can be injected into each of the electrode types before E_{mc} = 0.6 V is reached, i.e. before the evolution of H_2 gas would be expected if the electrode were to be polarized further [12]. In this experiment, the maximum voltage limit for Pt was used to compare only the relative capacitance of the two materials. Fig. 6, B shows the recorded voltage traces for each of the three materials during the constant current pulses shown in A, indicating where the maximum polarization voltage (E_{mc}) of 0.6 V is extracted from.

Accepted Manuscript

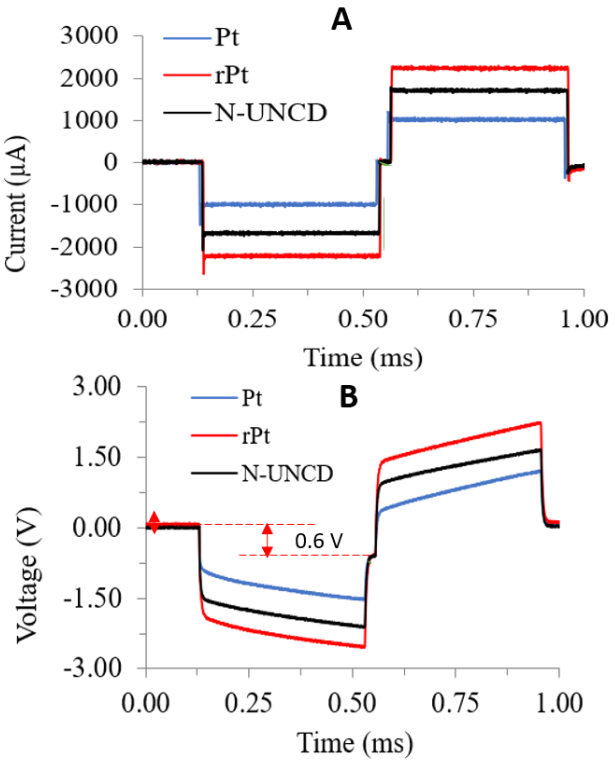

Fig. 6. A) Stimulator output trace showing the maximum, current amplitude deliverable through a Pt, rPt and N-UNCD electrode during a 400 µs per phase, constant current stimulation pulse, using the Pt maximum voltage limit of 0.6 V. B) The recorded electrode voltage excursion during the pulses depicted in A, The position where the E_{mc} voltage of 0.6 V is extracted is indicated on B. Electrodes were 1.0 mm in diameter and voltages are reported relative to an Ag/AgCl reference electrode. (Note: N-UNCD-O was not included in this figure)

Figure 7 shows measured Q_{inj} at a range of pulse durations for platinum (blue diamond), N-UNCD (black circle), rPt (red square), and N-UNCD-O (green cross). Also shown is a repeat measurement for N-UNCD-O after 5 days of continuous pulsing (black triangle) to demonstrate electrochemical robustness. Each data point is an average resulting from assessment of three identical electrodes. During these tests, an upper cathodic electrode polarization voltage limit of 1.0 V was used for N-UNCD [10, 11] and 0.6 V for platinum. The plot shows that N-UNCD-O electrodes displayed the highest Q_{inj} over all the phase durations measured (0.28 mC/cm^2, 100 µs; 1.01 mC/cm^2, 3200 µs). These values were at least double that of N-UNCD without oxygen plasma treatment at all phase durations and nearly triple that of rPt (0.09 mC/cm^2, 100 µs; 0.40 mC/cm^2, 3200 µs). Electrochemical stress testing did not lower capacitance, instead, a slight increase in Q_{inj} was observed following 5 days of constant pulsing.

Accepted Manuscript

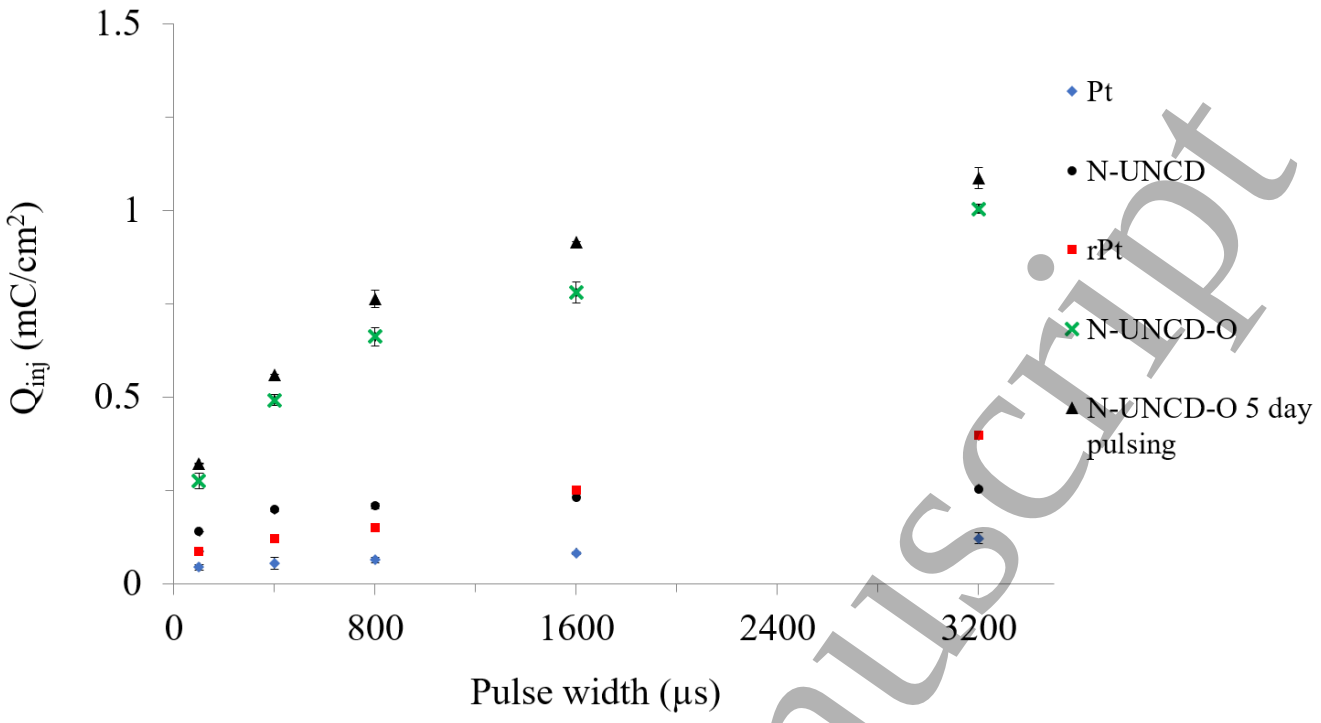

Fig. 7. Q_{inj} for Pt, rPt and N-UNCD and N-UNCD-O (before and after electrochemical stress test, n=3 electrodes for each case) at various phase durations. Error bars represent standar error of the mean.

The Q_{inj} for Pt, rPt and N-UNCD were also calculated following stress testing but are not shown in Fig. 7, for the sake of clarity. In brief, N-UNCD Q_{inj} did not change within error limits after stress testing, yielding values between 0.15 and 0.27 mC/cm^2 over the phase duration range. Bare platinum exhibited a substantial increase in Q_{inj} after pulsing. Rising from 0.1 mC/cm^2 to almost 0.2 mC/cm^2 for a 3200 µs per phase pulse. For rPt however, the Q_{inj} dropped from 0.4 mC/cm^2 to 0.27 mC/cm^2 when using a phase duration of 3200 µs after stress testing.

CVs and SEM images recorded before and after stress testing are shown in Fig. 8 for all samples. For platinum samples, there is clear evidence of changes in the CVs following stress testing. The appearance of the small anodic peaks due to hydrogen atom electroplating and the negative deflections due to dissolved oxygen reduction which occur at different potentials and peaks on the pristine samples, are absent after stress testing. Likewise, the SEM images reveal the appearance of etched pits, in particular on the smooth platinum samples. Etching was less evident on the rPt samples but detectable with close inspection, in particular as discoloration inside the smooth laser milled recesses. There were no discernable changes in the SEM images of N-UNCD or N-UNCD-O after stress testing. Compared to before and after CVs on platinum, The CVs of N-UNCD exhibited very little change after 5 days of pulsing. N-UNCD-O exhibited a drop in the area bounded by the CV after pulsing, which would normally indicate a drop in capacitance. This was not born out in the pulse test however where a small increase in Q_{inj} was recorded. Expanded electrochemical characterization is described elsewhere [29].

Accepted Manuscript

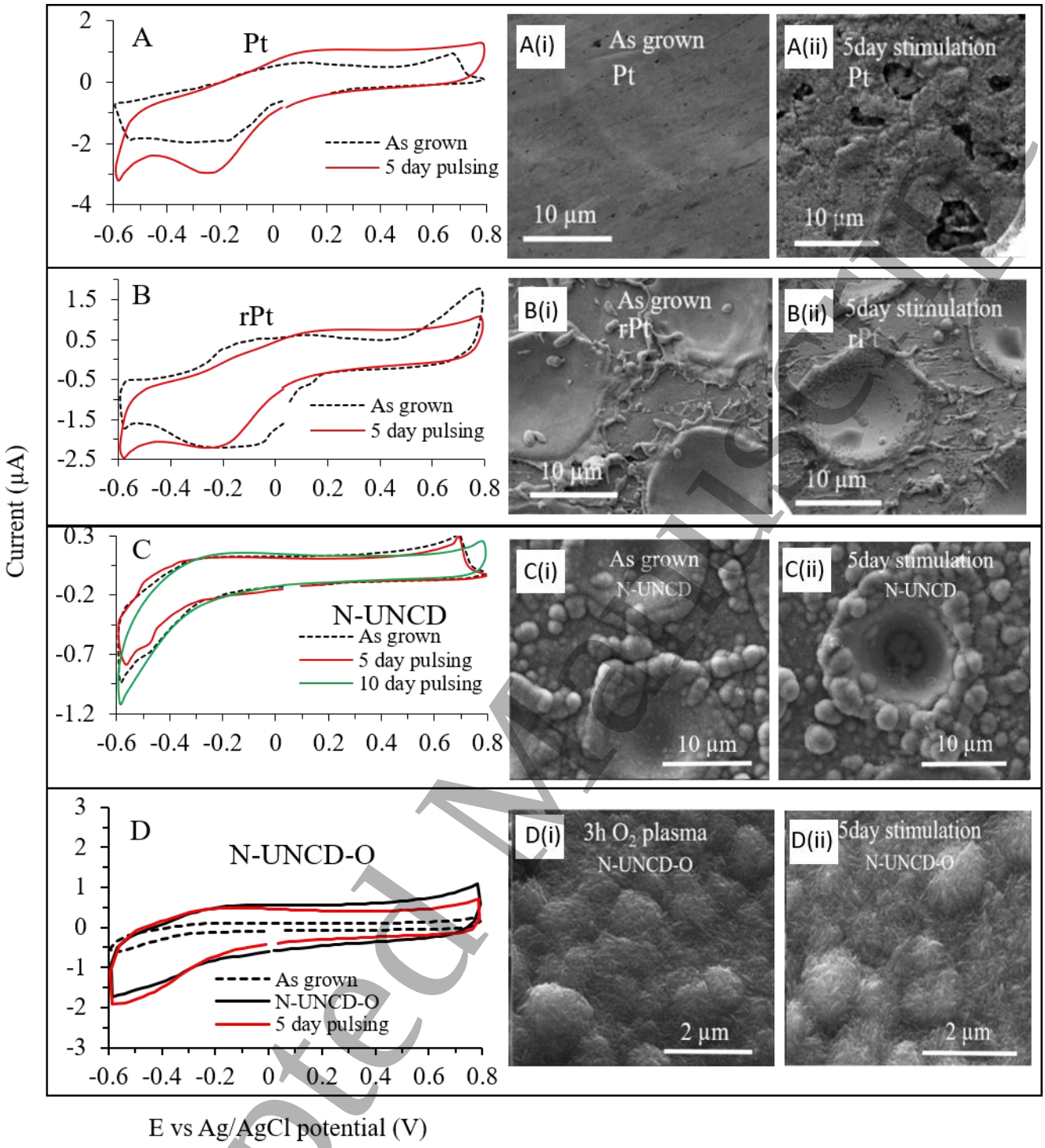

Fig. 8. CVs and SEM images of Pt (A-A(ii)), rPt (B-B(ii)), N-UNCD (C-C(ii)) and N-UNCD-O (D-D(ii)) for as-grown and following long-term stimulation cases.

4. Discussion

N-UNCD films grew conformally on roughened platinum substrates, leaving no obvious voids. In previous work, a growth rate of 0.5-1 µm/h is typical for the CVD system used hence films less than 3 µm in thickness were assumed

Accepted Manuscript

to have been obtained [21]. The inhomogeneity and mushroom shapes, evident in Fig. 8, C(i) and C(ii), are typical of N-UNCD films and are thought to arise from the growth of diamond, outward from aggregates of seeds. Due to the mismatch in thermal expansion coefficients between diamond and platinum, the foils became curved upon cooling (concave on the platinum side). This phenomenon could cause problems with large foils, perhaps forcing them to scroll. Foil squares, 5 mm square were slightly curved. Attempts to flatten the foils resulted in cracking of the diamond film. Delamination occurred on all but the 20 µm pitch roughened samples.

Sonication tests showed that the diamond films delaminated rapidly from flat sections of platinum between the laser milled pits. When the laser milled pits were sufficiently close to one another (20 µm), delamination due to sonication did not occur until 15 h and was minimal. Unlike other metals, platinum does not readily form a carbide [27, 30]. Heating of titanium for instance at even moderate temperatures such as 400 ºC is known to form a titanium carbide interlayer with diamond [31]. Platinum carbide is difficult to synthesize, occurring at 85 GPa and 2327 ºC [32]. Hence, a chemical attachment between diamond and platinum was not expected. Roughening of the platinum with closely spaced pits, however, led to more robust mechanical attachment of the diamond films, sufficient to survive 30 h of high energy sonication in water.

Consistent with previous work, N-UNCD exhibited a native capacitance roughly double that of platinum at short pulse times [33]. Roughened platinum outperformed N-UNCD at longer pulse lengths, most likely due to the surface-confined Faradaic reactions that are known to occur on platinum. With longer pulses, voltage excursions occur over a longer time period allowing more time for electrochemical processes [34-37]. During very short pulses, purely capacitive charging of the electrode dominates. It is likely that the diamond films have a short timeframe capacitance advantage due to possessing high nanoscale roughness (shown in Fig. 8 D2 and D3) which adds additional electrochemical surface area over the microscale roughness of the laser milled platinum substrate.

Also consistent with previous work, we found that oxygen plasma treatment of the diamond films resulted in a dramatic increase in electrochemical capacitance [22]. The large increase in area of the CV of N-UNCD-O (red trace) over N-UNCD (black trace) in Fig. 8, D1 illustrates this, with a maximum value reported here of 1 mC/cm^2 for 3200 µs. It remains unclear what the precise origins of the high capacitance are. It appears that it may be a combination of additional etching of the diamond surface generating higher surface area combined with surface oxidation changing the material's interaction with the aqueous electrolyte [10, 22]. As with our previous work, we observed no degradation in performance with extended use. Table 1 compares N-UNCD and N-UNCD-O from this work to a range of common and exotic charge injection materials.

Table 1. Comparison of proposed neural stimulation materials

Material	*Q_{inj} [mC/cm^2]*	*Water Window [V vs Ag | AgCl]*	*References*
Pt	0.1- 0.2 [a] [0.05-0.26]	-0.6 to 0.8	[38]
rPt	0.13 - 0.4 [a] [0.13-0.364]	-0.6 to 0.8	[38]
N-UNCD	0.15 - 0.27 [a] [0.1-0.2]	-1 to 1	[10, 11]
N-UNCD-O	0.6 – 1 [a] [1.2]	-1 to 1	[22]
CNTs	1-1.6	-1.5 to 1	[12]
BDD / CNTs	105	-1 to 1	[39]
PEDOT	15	-0.9 to 0.6	[19, 40]
Conducting Hydrogel	110	-0.8 to 0.6	[18]
Activated IrOx	1-5	-0.6 to 0.8	[12]
TiN	1	-0.8 to 1.1	[12]
BDD/TiN	1.8	-1.3 – 1.2	[41]
GO / PEDOT	1-4.5	-0.6 to 0.6	[42]
LCGO	43-60	-1 to 0.9	[38]

Accepted Manuscript

[a] Denotes results from this work, [ ] denotes results reported by others. LCGO (Liquid Crystal Graphene Oxide), GO (Graphene oxide), IrOx (Iridium oxide), TiN (Titanium Nitride), BDD (Boron-doped diamond), PEDOT (Poly (3,4-ethylene dioxythiophene)).

Materials with higher charge injection than N-UNCD-O have been reported. These typically have inherent surface confined Faradaic electrochemistry [12] or exceptionally high electrochemical surface area [18, 38, 39]. Iridium oxide and conducting polymers fit into the Faradaic charge transfer category [12]. Though promising, these materials are often not mechanically robust and can require specific electrochemical conditions to access their full potential. For instance, iridium oxide requires a bias voltage of 0.6 V be applied before the Faradaic processes that lead to high capacitance are activated. There is also evidence that the outstanding properties of iridium oxide *in vitro*, do not necessarily translate *in vivo* [43, 44]. This remains to be tested in the case of diamond. For conducting polymers such as Poly (3,4-ethylenedioxythiophene) (PEDOT) there are persistent biostability and hence longevity concerns [45-47]. Conducting hydrogels however, possess very high Q_{inj} and have shown good stability during long-term pulsing [18]. Graphene and carbon nanotube coatings lead to high charge injection capacity, but the coatings are famously delicate and friable [48, 49]. One notable exception exists in the work of Zanin *et al.* There, a carbon nanotube film was coated with BDD yielding a robust surface with capacitance ~450 times greater than that of the equivalent, flat BDD electrodes [39]. A similar approach was employed by Maijs *et al*. who grew boron doped diamond films over porous titanium nitride films [41].

The closest direct comparison to N-UNCD is titanium nitride (TiN), a material also deposited by chemical vapor deposition that operates by purely capacitive charge injection. TiN forms films with a columnar structure that have extremely high nanoscale roughness and hence high electrochemical surface area [12]. Charge injection values around 0.9 mC/cm^2 are typically reported for this material [50, 51]. TiN films are softer than diamond and suffer mechanical damage easily, but electrodes are well tolerated *in vivo* and can be patterned using common lithographic methods. Patterning of CVD diamond is more challenging, but methods have been developed, nevertheless. Girard *et al.* presented a method of patterned diamond deposition by pre-patterning the seeds from which the diamond was grown [52] and Ganesan *et al.* presented a method of patterning by laser ablation [53-55]. It should be noted that TiN deposition temperatures are much lower than diamond, typically 400 ºC [56], which means the technology can be applied directly onto a wider range of materials than N-UNCD. To employ diamond on low-temperature substrates, the diamond must be grown separately and transferred.

An important future consideration is that Q_{inj} stability of N-UNCD has not yet been assessed *in vivo*. Green et al. found that the Q_{inj} of roughened platinum was greatly reduced *in vivo* compared with *in vitro* [57]. This phenomonen may arise as a result of protein fouling or a confined electrochemical environment. Through some diamond electrodes have exhibited resistance to fouling in electrochemical sensing applications [58], they have not, as yet, been assessed specifically for stimulation stability *in vivo*.

Perhaps the most important advantage that diamond possesses, is excellent biocompatibility and very high electrochemical and biochemical stability [20]. For biomedical implants, there is a range of applications where surgical removal of devices is not feasible (such as an intracortical prosthesis for vision or somatosensory function) and hence the devices must last for a very long time in order to justify the risk to the patient and avoid re-implantation. In the case of retinal prostheses, devices should last for decades at least. The effects of electrochemical stress tests depicted in Fig. 8, demonstrate the exceptional stability of diamond films. Pitting, such as observed here, and gradual dissolution of platinum, operated at its limits, has been previously reported [59, 60]. N-UNCD appears to be impervious to electrochemical damage, within safe voltage limits. The stability of the high capacitance in the oxygen plasma activated N-UNCD-O samples is also notable. Above 1.0 V it is possible that some water oxidation might occur, leading to radicals that can interact with and functionalize the diamond surface. In previous work by Garrett *et al.* it was demonstrated that electrochemical oxidation is an alternative method for increasing charge injection capacity [11].

5. Conclusion

Accepted Manuscript

Diamond can be effectively deposited on Pt by using a laser roughening, pre-deposition process. The electrodes, once exposed to an oxygen plasma are stable, have high charge injection properties and would appear to be highly suited for neural stimulation implants. Sonication strongly indicates that roughening of the platinum substrate improves the adhesion of N-UNCD films significantly when a regular array of laser pits 20 µm in spacing was employed. Electrochemical tests established that N-UNCD grown on roughened platinum has comparable Q_{inj} to Pt and rPt. Once activated with oxygen plasma treatment, however, N-UNCD-O showed significantly enhanced electrochemical performance compared to Pt. In addition, the *in vitro* electrochemical stability assessment showed that N-UNCD and/or N-UNCD-O were more stable than Pt and roughened Pt.

6. Acknowledgments

Authors gratefully acknowledge Vanessa Maxim for her support this work to fabricate electrodes. (Funding: This research and KS were supported by an Australian Research Council (ARC) DECRA grant DE130100922. DJG is supported by the National Health and Medical Research Council (NHMRC) of Australia, grant GNT1101717. The Bionics Institute acknowledges the support received from the Victorian Government through its Operational Infrastructure Program for this work). SEM Imaging of electrodes was conducted at the Advanced Microscopy Facility at Bio21, (The University of Melbourne) on an FEI NOVA Nanolab. SP is shareholder, director and chief technology officer of iBIONICS, a company developing a diamond based retinal implant. SP and DG are shareholders in Carbon Cybernetics, a company developing a carbon-based neural interface.

7. References

[1] Zhou J J, Chen T S, Farber H, Shetter A G, Ponce F A 2018 Open-loop deep brain stimulation for the treatment of epilepsy: a systematic review of clinical outcomes over the past decade (2008-present) *Neurosurg. Focus* **45** 13

[2] Bina R W, Langevin J P 2018 Closed Loop Deep Brain Stimulation for PTSD, Addiction, and Disorders of Affective Facial Interpretation: Review and Discussion of Potential Biomarkers and Stimulation Paradigms *Front. Neurosci.* **12** 13

[3] Kundu B, Brock A A, Englot D J, Butson C R, Rolston J D 2018 Deep brain stimulation for the treatment of disorders of consciousness and cognition in traumatic brain injury patients: a review *Neurosurg. Focus* **45** 8

[4] Norman D J, Gonzalez-Fernandez E, Clavadetscher J, Tucker L, Staderini M, Mount A R, Murray A F, Bradley M 2018 Electrodrugs: an electrochemical prodrug activation strategy *Chem. Commun.* **54** 9242-9245

[5] Kumsa D W, Bhadra N, Hudak E M, Mortimer J T 2017 Electron transfer processes occurring on platinum neural stimulating electrodes: pulsing experiments for cathodic-first, charge-balanced, biphasic pulses for 0.566 <= k <= 2.3 in rat subcutaneous tissues *J. Neural Eng.* **14** 16

[6] Briggs R J S, Eder H C, Seligman P M, Cowan R S C, Plant K L, Dalton J, Money D K, Patrick J F 2008 Initial clinical experience with a totally implantable cochlear implant research device *Otol. Neurotol.* **29** 114-119

[7] Vaidya A, Borgonovi E, Taylor R S, Sahel J-A, Rizzo S, Stanga P E, Kukreja A, Walter P 2014 The cost-effectiveness of the Argus II retinal prosthesis in Retinitis Pigmentosa patients *BMC Ophthalmology* **14** 1-10

[8] Slutzky M W 2019 Brain-Machine Interfaces: Powerful Tools for Clinical Treatment and Neuroscientific Investigations *Neuroscientist* **25** 139-154

[9] Electrochemical Principles of Safe Charge Injection, Neurobionics: The Biomedical Engineering of Neural Prostheses.

[10] Garrett D J, Ganesan K, Stacey A, Fox K, Meffin H, Prawer S 2012 Ultra-nanocrystalline diamond electrodes: optimization towards neural stimulation applications *J. Neural Eng.* **9**

[11] Hadjinicolaou A E, *et al.* 2012 Electrical stimulation of retinal ganglion cells with diamond and the development of an all diamond retinal prosthesis *Biomaterials* **33** 5812-5820

[12] Cogan S F, Neural stimulation and recording electrodes, Annual Review of Biomedical Engineering, Annual Reviews, Palo Alto, 2008, pp. 275-309.

[13] Kumsa D W, Bhadra N, Hudak E M, Kelley S C, Untereker D F, Mortimer J T 2016 Electron transfer processes occurring on platinum neural stimulating electrodes: a tutorial on the i(V-e) profile *J. Neural Eng.* **13** 15

Accepted Manuscript

[14] Corna A, Herrmann T, Zeck G 2018 Electrode-size dependent thresholds in subretinal neuroprosthetic stimulation *J. Neural Eng.* **15** 11
[15] Cogan S F, Ludwig K A, Welle C G, Takmakov P 2016 Tissue damage thresholds during therapeutic electrical stimulation *J. Neural Eng.* **13** 13
[16] Shannon R V 1992 A model of safe levels for electrical-stimulation *IEEE Trans. Biomed. Eng.* **39** 424-426
[17] Ivanovskaya A N, Belle A M, Yorita A M, Qian F, Chen S P, Tooker A, Lozada R G, Dahlquist D, Tolosa V 2018 Electrochemical Roughening of Thin-Film Platinum for Neural Probe Arrays and Biosensing Applications *J. Electrochem. Soc.* **165** G3125-G3132
[18] Staples N A, Goding J A, Gilmour A D, Aristovich K Y, Byrnes-Preston P, Holder D S, Morley J W, Lovell N H, Chew D J, Green R A 2018 Conductive Hydrogel Electrodes for Delivery of Long-Term High Frequency Pulses *Front. Neurosci.* **11**
[19] Aregueta-Robles U A, Woolley A J, Poole-Warren L A, Lovell N H, Green R A 2014 Organic electrode coatings for next-generation neural interfaces *Frontiers in Neuroengineering* **7**
[20] Garrett D J, Saunders A L, McGowan C, Specks J, Ganesan K, Meffin H, Williams R A, Nayagam D A X 2015 In vivo biocompatibility of boron doped and nitrogen included conductive-diamond for use in medical implants *Journal of Biomedical Materials Research Part B: Applied Biomaterials* n/a-n/a
[21] Ganesan K, Garrett D J, Ahnood A, Shivdasani M N, Tong W, Turnley A M, Fox K, Meffin H, Prawer S 2014 An all-diamond, hermetic electrical feedthrough array for a retinal prosthesis *Biomaterials* **35** 908-915
[22] Tong W*, et al.* 2016 Optimizing growth and post treatment of diamond for high capacitance neural interfaces *Biomaterials* **104** 32-42
[23] Hadjinicolaou A E, Savage C O, Apollo N V, Garrett D J, Cloherty S L, Ibbotson M R, O'Brien B J 2015 Optimizing the Electrical Stimulation of Retinal Ganglion Cells *Neural Systems and Rehabilitation Engineering, IEEE Transactions on* **23** 169-178
[24] Shivdasani M, Garrett D, Nayagam D, Villalobos J, Allen P, Saunders A, McPhedran M, McGowan C, Meffin H, Shepherd R 2013 In Vivo Electrical Stimulation of a Retinal Prosthesis Containing Conductive Diamond Electrodes *Investigative Ophthalmology & Visual Science* **54** 1029-1029
[25] Fhaner M, Zhao H, Bian X C, Galligan J J, Swain G M 2011 Improvements in the formation of boron-doped diamond coatings on platinum wires using the novel nucleation process (NNP) *Diam. Relat. Mat.* **20** 75-83
[26] Cvacka J, Quaiserova V, Park J, Show Y, Muck A, Swain G M 2003 Boron-doped diamond microelectrodes for use in capillary electrophoresis with electrochemical detection *Anal. Chem.* **75** 2678-2687
[27] Tachibana T, Yokota Y, Miyata K, Kobashi K, Shintani Y 1997 Heteroepitaxial diamond growth process on platinum (111) *Diamond and Related Materials* **6** 266-271
[28] Jiang N, Wang C L, Won J H, Joen M H, Mori Y, Hatta A, Ito T, Sasaki T, Hiraki A 1997 Interface characterization of chemical-vapour-deposited diamond on Cu and Pt substrates studied by transmission electron microscopy *Appl. Surf. Sci.* **117** 587-591
[29] Sikder M K U, Exploring the use of diamond in medical implants, 2018.
[30] Harris S J, Belton D N, Weiner A M, Schmieg S J 1989 Diamond formation on platinum *Journal of applied physics* **66** 5353-5359
[31] Fu Y, Du H, Sun C Q 2003 Interfacial structure, residual stress and adhesion of diamond coatings deposited on titanium *Thin solid films* **424** 107-114
[32] Ono S, Kikegawa T, Ohishi Y 2005 A high-pressure and high-temperature synthesis of platinum carbide *Solid state communications* **133** 55-59
[33] Hadjinicolaou A E, Leung R T, Garrett D J, Ganesan K, Fox K, Nayagam D A, Shivdasani M N, Meffin H, Ibbotson M R, Prawer S 2012 Electrical stimulation of retinal ganglion cells with diamond and the development of an all diamond retinal prosthesis *Biomaterials* **33** 5812-5820
[34] Leung R T, Shivdasani M N, Nayagam D A, Shepherd R K 2015 In vivo and in vitro comparison of the charge injection capacity of platinum macroelectrodes *IEEE Trans Biomed Eng* **62** 849-857
[35] Aregueta-Robles U A, Woolley A J, Poole-Warren L A, Lovell N H, Green R A 2014 Organic electrode coatings for next-generation neural interfaces *Frontiers in neuroengineering* **7**

Accepted Manuscript

[36] Negi S, Bhandari R, Rieth L, Solzbacher F 2010 In vitro comparison of sputtered iridium oxide and platinum-coated neural implantable microelectrode arrays *Biomedical materials* **5** 015007
[37] Cogan S F, Troyk P R, Ehrlich J, Plante T D 2005 In vitro comparison of the charge-injection limits of activated iridium oxide (AIROF) and platinum-iridium microelectrodes *IEEE Transactions on Biomedical Engineering* **52** 1612-1614
[38] Apollo N V, Maturana M I, Tong W, Nayagam D A X, Shivdasani M N, Foroughi J, Wallace G G, Prawer S, Ibbotson M R, Garrett D J 2015 Soft, Flexible Freestanding Neural Stimulation and Recording Electrodes Fabricated from Reduced Graphene Oxide *Adv. Funct. Mater.* **25** 3551-3559
[39] Zanin H, May P W, Fermin D J, Plana D, Vieira S M C, Milne W I, Corat E J 2014 Porous Boron-Doped Diamond/Carbon Nanotube Electrodes *Acs Applied Materials & Interfaces* **6** 990-995
[40] Green R A, Matteucci P B, Hassarati R T, Giraud B, Dodds C W D, Chen S, Byrnes-Preston P J, Suaning G J, Poole-Warren L A, Lovell N H 2013 Performance of conducting polymer electrodes for stimulating neuroprosthetics *J. Neural Eng.* **10** 11
[41] Meijs S*, et al.* 2018 Diamond/Porous Titanium Nitride Electrodes With Superior Electrochemical Performance for Neural Interfacing *Front. Bioeng. Biotechnol.* **6** 10
[42] Tian H C*, et al.* 2014 Graphene oxide doped conducting polymer nanocomposite film for electrode-tissue interface *Biomaterials* **35** 2120-2129
[43] Weiland J D, Anderson D J 2000 Chronic neural stimulation with thin-film, iridium oxide electrodes *IEEE Trans. Biomed. Eng.* **47** 911-918
[44] Cogan S F, Guzelian A A, Agnew W F, Yuen T G, McCreery D B 2004 Over-pulsing degrades activated iridium oxide films used for intracortical neural stimulation *Journal of neuroscience methods* **137** 141-150
[45] Cui X T, Zhou D D 2007 Poly (3, 4-ethylenedioxythiophene) for chronic neural stimulation *Neural Systems and Rehabilitation Engineering, IEEE Transactions on* **15** 502-508
[46] Wilks S J, Richardson-Burns S M, Hendricks J L, Martin D C, Otto K J 2009 Poly (3, 4-ethylenedioxythiophene) as a micro-neural interface material for electrostimulation *Frontiers in neuroengineering* **2**
[47] Green R A, Hassarati R T, Bouchinet L, Lee C S, Cheong G L, Jin F Y, Dodds C W, Suaning G J, Poole-Warren L A, Lovell N H 2012 Substrate dependent stability of conducting polymer coatings on medical electrodes *Biomaterials* **33** 5875-5886
[48] Clancy A J, Bayazit M K, Hodge S A, Skipper N T, Howard C A, Shaffer M S 2018 Charged Carbon Nanomaterials: Redox Chemistries of Fullerenes, Carbon Nanotubes, and Graphenes *Chemical reviews* **118** 7363-7408
[49] Baughman R H, Zakhidov A A, De Heer W A 2002 Carbon nanotubes--the route toward applications *science* **297** 787-792
[50] Weiland J D, Anderson D J, Humayun M S 2002 In vitro electrical properties for iridium oxide versus titanium nitride stimulating electrodes *Biomedical Engineering, IEEE Transactions on* **49** 1574-1579
[51] Cogan S F 2008 Neural stimulation and recording electrodes *Annu. Rev. Biomed. Eng.* **10** 275-309
[52] Girard H A, Perruchas S, Gesset C, Chaigneau M, Vieille L, Arnault J-C, Bergonzo P, Boilot J-P, Gacoin T 2009 Electrostatic grafting of diamond nanoparticles: a versatile route to nanocrystalline diamond thin films *ACS applied materials & interfaces* **1** 2738-2746
[53] Vinodkumar R, Navas I, Chalana S, Gopchandran K, Ganesan V, Philip R, Sudheer S, Pillai V M 2010 Highly conductive and transparent laser ablated nanostructured Al: ZnO thin films *Applied Surface Science* **257** 708-716
[54] Beena D, Lethy K, Vinodkumar R, Pillai V M, Ganesan V, Phase D, Sudheer S 2009 Effect of substrate temperature on structural, optical and electrical properties of pulsed laser ablated nanostructured indium oxide films *Applied Surface Science* **255** 8334-8342
[55] Lethy K, Beena D, Kumar R V, Pillai V M, Ganesan V, Sathe V 2008 Structural, optical and morphological studies on laser ablated nanostructured WO3 thin films *Applied Surface Science* **254** 2369-2376
[56] Kurtz S R, Gordon R G 1986 Chemical vapor deposition of titanium nitride at low temperatures *Thin Solid Films* **140** 277-290

Accepted Manuscript

[57] Green R A, Matteucci P B, Dodds C W D, Palmer J, Dueck W F, Hassarati R T, Byrnes-Preston P J, Lovell N H, Suaning G J 2014 Laser patterning of platinum electrodes for safe neurostimulation *J. Neural Eng.* **11** 17
[58] Macpherson J V 2015 A practical guide to using boron doped diamond in electrochemical research *Physical Chemistry Chemical Physics* **17** 2935-2949
[59] Shepherd R K, Murray, M. T., Houghton, M. E. and Clark G. M. 1985 Scanning electron microscopy of chronically stimulated platinum intracochlear electrodes *Biomaterials* **6** 237-242
[60] Green R, Matteucci P, Dodds C, Palmer J, Dueck W, Hassarati R, Byrnes-Preston P, Lovell N, Suaning G 2014 Laser patterning of platinum electrodes for safe neurostimulation *Journal of neural engineering* **11** 056017

Accepted Manuscript